Microfluidic Templated Multicompartment Microgels for 3D Encapsulation and Pairing of Single Cells

Liyuan Zhang, Kaiwen Chen, Haoyue Zhang, Bo Pang, Chang-Hyung Choi, Angelo S. Mao, Hongbing Liao, Stefanie Utech, David J. Mooney, Huanan Wang,* and David A. Weitz*

Controlled encapsulation and pairing of single cells within a confined 3D matrix can enable the replication of the highly ordered cellular structure of human tissues. Microgels with independently controlled compartments that can encapsulate cells within separately confined hydrogel matrices would provide precise control over the route of pairing single cells. Here, a one-step microfluidic method is presented to generate monodisperse multicompartment microgels that can be used as a 3D matrix to pair single cells in a highly biocompatible manner. A method is presented to induce microgels formation on chip, followed by direct extraction of the microgels from oil phase, thereby avoiding prolonged exposure of the microgels to the oil. It is further demonstrated that by entrapping stem cells with niche cells within separate but adjacent compartments of the microgels, it can create complex stem cell niche microenvironments in a controlled manner, which can serve as a useful tool for the study of cell–cell interactions. This microfluidic technique represents a significant step toward high-throughput single cells encapsulation and pairing for the study of intercellular communications at single cell level, which is of significant importance for cell biology, stem cell therapy, and tissue engineering.

Human tissues are composed of different cells that assemble, coordinate, and interact with one another in a hierarchically organized manner to achieve tissues-specific functions. The interactions between these cells are important in regulating cell behavior by biochemical signaling cues from neighboring cells. To study the intercellular regulatory network in tissues or organs, coculture of different cells in vitro has been a widely used approach. However, conventional bulk coculture methods on polystyrene or glass surfaces do not reveal the underlying mechanism of cell–cell interactions as they cannot precisely control and assemble different cells in vitro and replicate the cellular structure of natural tissues at microscale. Cells grown on surfaces are dramatically different as compared to the cells grown in natural 3D cellular microenvironment in vivo; moreover, single cell–cell interactions cannot be distinguished from the collective behavior.[1] As an alternative to bulk coculture methods, miniaturization techniques that can be used to mimic the cellular microenvironment by precise manipulation and assembly of cells within a confined micrometer-sized volume have been developed using microfluidic channels or microwells.[1b,2] Multicompartment microgels with independently controlled compartments that each can encapsulate different cargos within a hydrogel matrix would be a promising approach for the study of paired cells of different types.[3] The inherent microporosity, biocompatibility, and similarity to natural extracellular matrix of microgels render them capable of regulating cell behavior by biophysical and biochemical signaling cues.[4] Therefore, techniques including microfluidic approaches,[3e,h] flow lithography,[5] and centrifuge-based

Dr. L. Zhang, K. Chen, H. Zhang, B. Pang, Prof. H. Wang
School of Life Science and Biotechnology
Dalian University of Technology
Dalian 116023, P. R. China
E-mail: huananwang@dlut.edu.cn

Dr. L. Zhang, Prof. C.-H. Choi, Dr. A. S. Mao, Dr. S. Utech,
Prof. D. J. Mooney, Prof. D. A. Weitz
School of Engineering and Applied Science
Harvard University
9 Oxford St, Cambridge, MA 02138, USA
E-mail: weitz@seas.harvard.edu

B. Pang, H. Liao
College of Stomatology
Guangxi Medical University
Nanning 530021, P. R. China

Dr. A. S. Mao, Prof. D. J. Mooney, Prof. D. A. Weitz
Wyss Institute for Biologically Inspired Engineering
Harvard University
3 Blackfan Cir, Boston, MA 02115, USA

Prof. D. A. Weitz
Department of Physics
Harvard University
9 Oxford St, Cambridge, MA 02138, USA

ADVANCED
SCIENCE NEWS
www.advancedsciencenews.com

NANO MICRO
small
www.small-journal.com

methods[3c] have been developed to generate multicompartment microgels; these methods either sequentially fabricate microgels as modules to assemble into the desired structure, or simultaneously solidify multiple components to form a multicompartment microgel. However, their widespread application for cell encapsulation and pairing is limited due to the reduced cell viability resulting from the harsh gelation process,[3c] the poor efficiency and precision in pairing different cells,[2b] and the difficulty in assembly cells at single cell level.[3c] Therefore, a technique that enables single-cell encapsulation and pairing in a controllable and biocompatible manner would be highly valuable for the study of regulatory signaling cues between cells.

Herein, we present a microfluidic method for producing monodisperse multicompartment microgels with independently controlled compartments that each entraps single cells and enables controlled assembly of these cells within a confined 3D micrometer-sized space. We produce compartmentalized microgels through rapid gelation of multiple hydrogel precursor aqueous solutions. The microgels are immediately transferred from the oil in which they are formed to an aqueous continuous phase by destabilizing the oil–water interface on chip through dissociating the surfactants. This approach leads to continuous generation of multicompartment microgels while retaining cell viability by substantially reducing the resident time of cells within the emulsion. We further demonstrate that by entrapping stem cells with niche cells within separate compartments of the microgels, we can pair single cells and create complex stem cell niche microenvironments in a controlled manner for the in vitro study of the effect niche environment on stem cell fate.
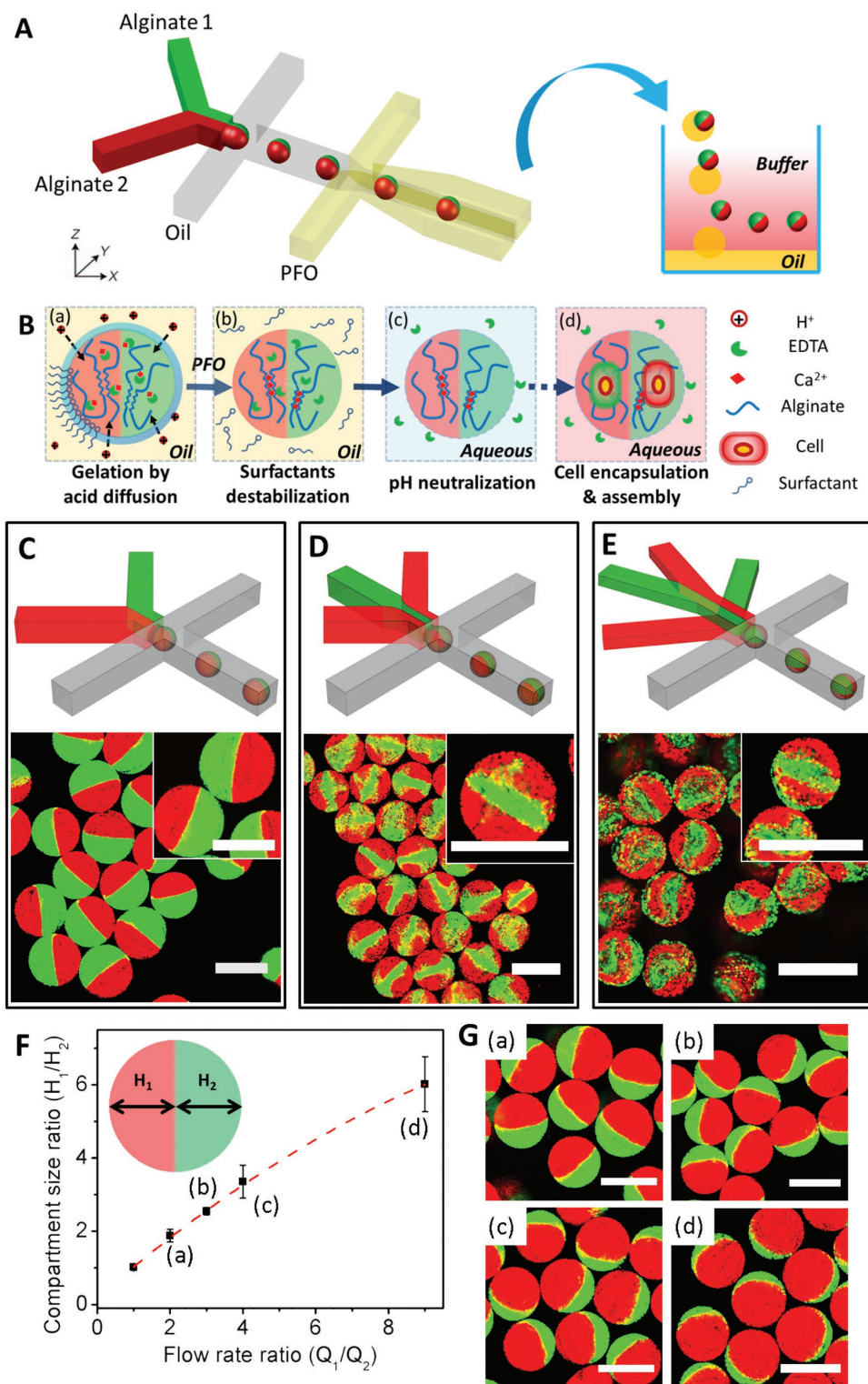
To produce multicompartment microgels, we use a flow-focusing PDMS (polydimethylsiloxane, Sylgard 184, Dow Corning, Midland, MI, USA) microfluidic device to generate monodisperse aqueous droplets containing multiphase alginate solutions as templates (**Figure 1**A). We inject 1 w/v% alginate solutions (in minimum essential medium) containing 50×10^{-3} M calcium-ethylenediaminetetracetic acid (Ca-EDTA) complex as the dispersed phase and fluorocarbon oil (HFE7500, Novec 7500 Engineered Fluid) containing 1% Krytox-polyethylene glycol (PEG)-Krytox surfactant and 0.1% acetic acid as the continuous phase. After the generation of alginate droplets, acetic acid in the oil phase diffuses into the droplets triggering the release of calcium from the Ca-EDTA. Rapid gelation reaction occurs immediately upon contact of alginate and calcium ions, thus enabling the production of multicompartment microgels (Figure 1B).[6] To neutralize the acetic acid, which is cytotoxic, we first redisperse the microgel in an aqueous buffer by destabilizing the oil–water interface. We accomplish this by introducing an additional channel to inject 1H,1H,2H,2H-perfluoro-1-octanol (PFO, Alfa Aesar) after the microgel formation. The PFO reduces the stability of the oil–water interface by dissociating the surfactants.[7] Once the oil–water interface is destabilized, the microgels are immediately transferred from the oil to an aqueous phase consisting of a 25×10^{-3} M HEPPES (4-(2-Hydroxyethyl)piperazine-1-ethanesulfonic acid (Sigma, 83264-100ML-F)) buffer (Figure 1Bc), further neutralizing the pH within the microgels. The formation of multicompartment microgels and subsequent neutralization of the acetic acid is accomplished in a single microfluidic device, thereby minimizing the exposure time of the microgels to harsh acidic conditions. This feature is crucial to ensure cells are encapsulated in the microgels in a biocompatible manner (Figure 1Bd).
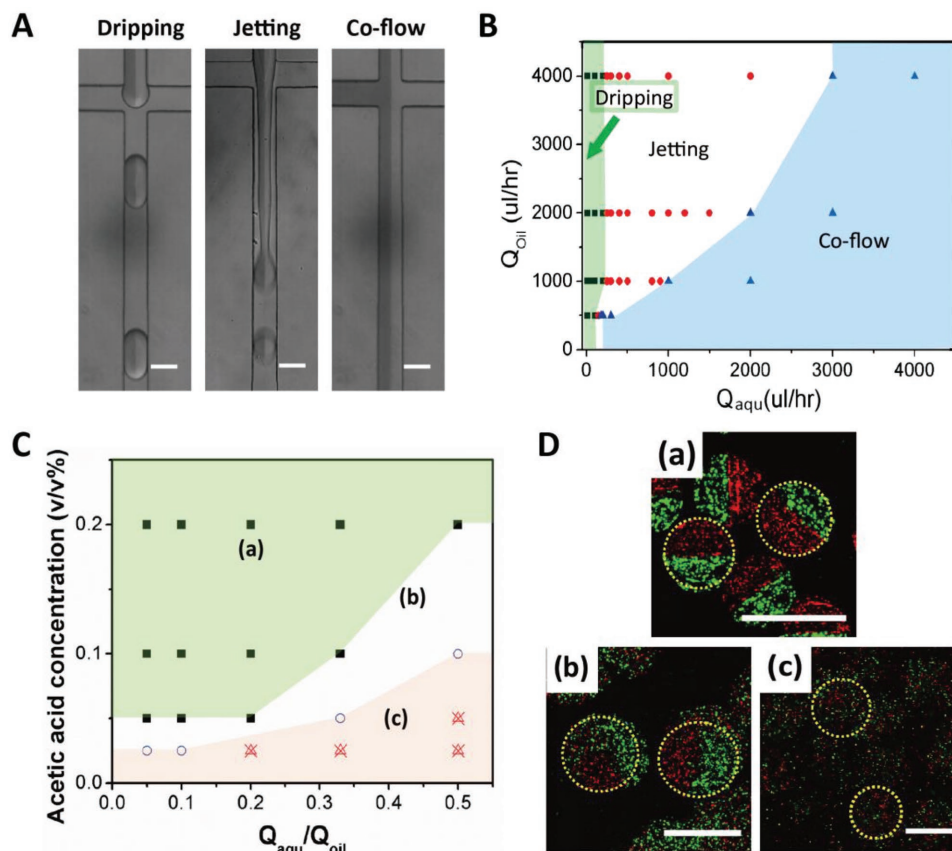
By utilizing drop makers with different geometries (Figure S1, Supporting Information), we can produce microgels with up to four compartments as shown in Figure 1C–E. To clearly visualize each compartment, we incorporate fluorescein or rhodamine-labeled polystyrene nanoparticles (200 nm) into each alginate phase. The sharp interface between distinct compartments is a consequence of rapid Ca-alginate gelation. In liquid droplets formed with microfluidic devices, internal convective flows, induced by the unavoidable shear stresses during droplet formation, accelerate mixing between the initially distinct compartments.[8] However, the rapid Ca-alginate gelation essentially eliminates these convective flows during droplet formation. With convective flows eliminated, mixing times are determined by much slower interdiffusion between solid gel phases; this diffusive mixing is sufficiently slow to ensure sharp interfaces and distinct compartments. In addition to generating multiple and distinct compartments, we can precisely control the relative volumes of each compartments by tuning the flow rate ratio of the input alginate solutions, as shown in Figure 1F,G. Compared to previous techniques for fabricating multicompartment microgels, our approach integrates microgel formation and redispersion in aqueous phase while neutralizing cytotoxic reaction agents into one-step process. This greatly simplifies the approach and could potentially allow the scale up of encapsulation.

We further study the fabrication parameters for producing monodisperse Janus microgels. Three different flow patterns can be formed by tuning aqueous phase flow rate Q_{aqu} and oil phase flow rate Q_{oil}. These include dripping, jetting, and coflow as shown in **Figure 2**A. The flow rate regimes for different flow patterns are shown Figure 2B. Differently colored areas represent different regimes. Droplets are uniformly formed at small Q_{aqu}. When Q_{aqu} increases, uniform microgels can be formed at the jetting regime. For high Q_{aqu}, biphasic laminar flow occurs and no drops are formed. We can obtain microgels in the dripping and jetting regimes. In addition to the microgels formation, the acetic acid concentration plays an important role in microstructure of as-prepared Janus microgel, as shown in Figure 2C. At acetic acid concentration larger than 0.2%, Janus microgels with a sharp interface are produced at varied flow rate ratio of Q_{aqu}/Q_{oil}, which corresponds with Figure 2Da. As the acetic acid concentration decreases gradually, the interface within microgels becomes unclear, shown in Figure 2Db. When the acid concentration decreases further, we no longer produce well-defined microgels, as shown in Figure 2Dc. Differently colored areas in Figure 2C represent these three microgels formation stages in Figure 2D, respectively. These results indicate that multicompartment microgels with a clear interface can be fabricated with adequate acetic acid to induce fast gelation and to avoid extensive diffusion between neighboring flows.

Conventional methods for generation cell-laden microgels are usually based on water-in-oil emulsion droplet technique, in which cells are usually generated in nutrient and oxygen-depleted environment and/or cross-linking agent/surfactant-enriched oil phase. Therefore, the exposure to oil should be minimized to reduce cellular injuries during the generation, operation, and collection of microgels.[6] Conventionally, microgels are first generated on chip and then transferred from

ADVANCED
SCIENCE NEWS
www.advancedsciencenews.com

NANO MICRO
small
www.small-journal.com

Figure 1. One-step microfluidic generation of multicompartment microgels for controlled cell encapsulation and assembly. A) Schematic illustration shows PDMS microfluidic device for the production of single emulsion drops consisting of multiple aqueous phases. The alginate droplets are solidified via on-chip gelation and immediately collected into aqueous solution (cell media) after dissociating of surfactants by coflowing PFO. B) Schematic illustration showing the detailed mechanism to form multicompartment alginate microgels as shown in Figure Ba–d. Figure Bd is the example when using Janus microgel to assembly cells in each compartment. C–E) Representative fluorescent microscopic image showing multicompartment microgels with C) bi-, D) tri-, and E) quadri-compartment microgels by utilizing microfluidic devices with different numbers of injection channel. Fluorescein (green)- or rhodamine (red)-labeled polystyrene nanoparticles (diameter: 200 nm; concentration: 0.2 vol%) in the alginate phase to facilitate visualization. F) The varying size ratio of each compartment in Janus microgels as a function of the flow rate ratio of alginate solution phases (Q_1 and Q_2). G) Corresponding confocal images showing the Janus microgels with tunable compartment size ratio as shown in (F). Scale bars are 100 μm.

ADVANCED
SCIENCE NEWS
www.advancedsciencenews.com

NANO MICRO
small
www.small-journal.com

Figure 2. In-depth study of fabrication parameters for stable multicompartment microgels. A) Microscope images showing flow patterns generated in the microfluidic device for producing Janus microgels. B) Phase diagram showing flow conditions for stable formation of multicompartment microgels. Square, circle, and triangle denotes dripping, jetting, and coflow, respectively. Green square, red circle, and blue triangle are the data points of Q_{aqu} corresponding to Q_{oil}. C) Optimal condition of acetic acid concentration and flow rate ratio Q_{aqu}/Q_{oil} for stable formation of multicompartment microgels. Symbols represent data points of flow rate and acetic acid concentration. D) Confocal microscopy images of (a) symmetric Janus microgels with a sharp interface, (b) Janus microgels with an unclear interface, and (c) noncompartment microgels, corresponding to different regimes in (C). Scale bars are 100 μm.

oil into aqueous solution by multiple off-chip centrifugation washing steps. These time- and labor-consuming procedures, however, would result in aggregation of microgels, low retrieval efficiency, and compromised cell viability.[6c,d,9] This diminishes the potential of these methods being applied for high-throughput cell encapsulation. In addition, a harsh gelation process must be used to accelerate solidification of the compartments, which can cause cytotoxicity. Specifically, to generate cell-laden alginate microgels, a two-step method has to use acid to trigger-release calcium ions from Ca-EDTA[6a] or CaCO$_3$ nanoparticles[6b] to allow on-chip formation of microgels followed by a second step to transfer microgels into aqueous phase and neutralize pH off chip; this leads to low cell viability due to prolonged exposure of cells to acid (**Figure 3**A).

Therefore, one-step on-chip fabrication approaches have been proposed to timely extract microgels from oil into aqueous phase. However, so far, there is very limited literature on one-step microencapsulation methods for generation of cell-laden microgels. A one-step method for the generation of cell-laden microgels has been proposed using ultrathin shell double emulsion droplets as templates.[10] Nevertheless, the presence of oil shell prevents the diffusion of chemical cross-linking

agents and limits the gelation methods for aqueous microgels. Alternative approaches to extract microgels from oil to aqueous phase by depletion of carrier oil phase,[6d] mechanical filter gate,[6c] interfacial tension-based extraction,[6e] or dielectrophoresis-based extraction.[6f] However, these methods demand complicated device design that increases the system complexity and operational difficulty,[6c,d] and the microgels need to satisfy certain criteria of size and mechanical strength,[6e] or application of potentially cytotoxic electric field.[6f]

Here, using the one-step approach, we minimize the residential time of the microgels in harsh conditions and thereby reduce the cytotoxicity, as evidenced by the retained cell viability (NIH3T3 fibroblast cells) in contrast to the two-step microencapsulation approach[6a,9b,11] (Figure 3A). We further investigate the effect of acetic acid and Q_{aqu}/Q_{oil} on cell viability, shown in Figure 3B. We observe reduced cell viability upon decreasing Q_{oil} at constant $Q_{aqu} = 100$ μL h^{-1}, which is caused by the prolonged exposure time of cells to the oil phase before being transferred to the aqueous buffer. We obtain high cell viability upon increasing Q_{oil} at a constant Q_{aqu}, and only a concentration of acetic acid with minimal effect on cell viability is used for subsequent cell encapsulation experiment. Moreover, by using arginine-glycine-aspartic

ADVANCED
SCIENCE NEWS
www.advancedsciencenews.com

NANO | MICRO
small
www.small-journal.com
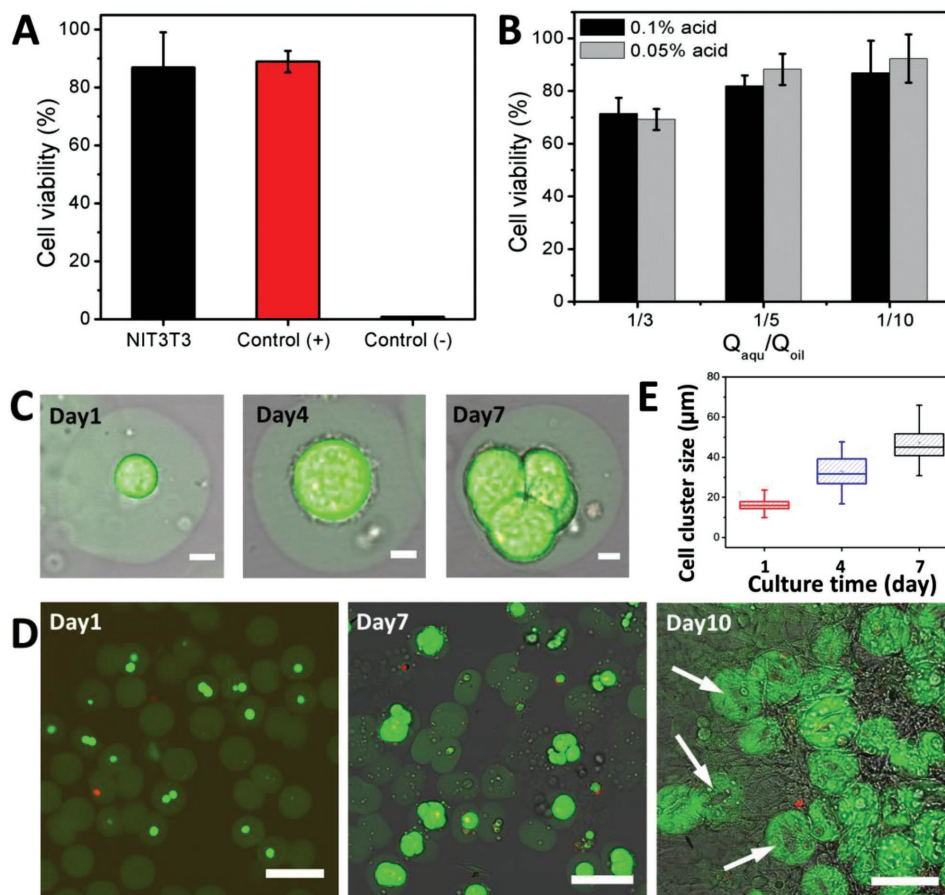
Figure 3. One-step generation of cell-laden microgels in a biocompatible manner. A) The viability of NIH3T3 cells after encapsulation using our one-step approach in comparison to conventional two-step microfluidic method and cells cultured on tissue culture plate (denoted as TCP). In the two-step method, cell-laden microgels are prepared based on previous method reported by Utech et al.;[6a] acetic acid is added in the oil phase to trigger-release calcium ions from Ca-EDTA upon droplet formation. Microgels are first formed on-chip and collected for 30 min, followed by the second off-chip washing step to transfer them into aqueous phase. B) The viability of NIH3T3 cells in the microgels as a function of acetic acid and flow rate ratios (Q_{aqu}/Q_{oil}) in which Q_{aqu} is 100 µL h^{-1}. C,D) The representative confocal microscopic images of C) high and D) low magnitude showing NIH3T3 fibroblasts encapsulated in RGD-alginate microgels at different time point of in vitro culture. Calcein and ethidium homodimer are used for staining live and dead cells, respectively. Alginate molecules are labelled by fluorescein. NIH3T3 cells continuously proliferate inside the microgels and eventually egress out of the microgels. At day 10, egressed cells colonize the surface of culture plates, leaving cracks on the microgels (denoted by white arrows). C) Scale bars = 10 µm. D) Scale bars = 100 µm. E) The average diameter of cell clusters within the microgels at different time point during in vitro culture.

acid (RGD)-modified alginate for cell encapsulation, we observe NIH3T3 cells continuously proliferate inside the microgels and eventually egress out of the microgels, and colonize the surface of culture plates (Figure 3C,D, Figure S2, Supporting Information). We evaluate cell proliferation by monitoring the average size of cell clusters (Figure 3E) and average cell number within microgels (Figure S3, Supporting Information) as a function of time. Moreover, we study the viability of mesenchymal stem cells (MSCs) and human umbilical vein endothelial cells (HUVECs) after being encapsulated in RGD-alginate microgels, as shown in **Figure 4**A,B. For MSCs, we observe continuous cell proliferation inside the microgels as evidenced by the size increase of cell clusters. In contrast, we observe that HUVECs remain viable but do not show obvious change in cell cluster size during 3D culture in alginate microgels, indicating these cells do not proliferate in alginate matrix; this might relate to the higher stiffness but less degradability of alginate matrix compared to more

physiologically relevant matrix such as collagen and gelatin which have been proven to support HUVECs spreading, proliferation, and vascularization in vitro.[12]

We further demonstrate the feasibility of using multicompartment microgels to pair single cells. We disperse NIH3T3 cell labeled with either fluorescent green or red dye (Green and red CellTracker, Thermo Fisher Scientific,) in RGD-alginate and use this as the dispersed phases to form Janus microgels. To distinguish each compartment, the different alginate compartments are also labeled, using fluorescein for the red dyed cells and rhodamine for the green dyed cell. By fine tuning the fabrication parameters including droplet size, flow rate, and initial cell concentration, we can produce Janus microgels that allow the distribution of different single cells in the separated compartment as shown in Figure 4C,D. The percentage of Janus microgels denoted as f(AB) simultaneously containing both cell types in each compartment can be approximated by

ADVANCED
SCIENCE NEWS
www.advancedsciencenews.com

NANO · MICRO
small
www.small-journal.com
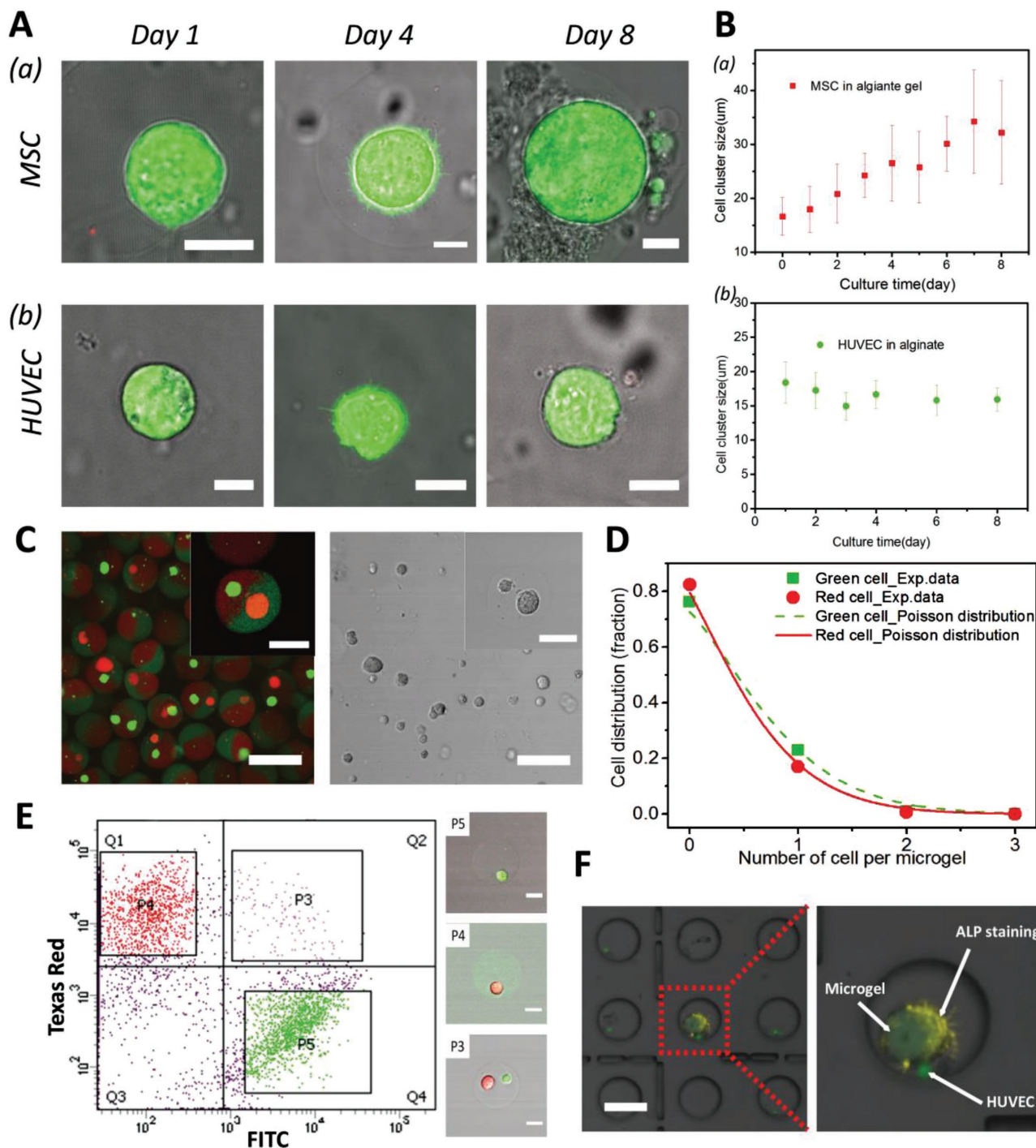
Figure 4. 3D encapsulation and pairing of single cells using multicompartmental microgels for the study of cell–cell interactions. A) The confocal microscopic images of MSCs (a) or HUVECs (b) encapsulated in RGD-alginate microgels with single compartment at different time point of in vitro culture. Calcein and ethidium homodimer are used for staining live and dead cells, respectively. Alginate molecules are labelled by fluorescein. Scale bars are 10 μm. B) The change of average diameters of cell clusters formed by MSC (a) or HUVEC (b) in the microgels at different time point of in vitro culture. C) Confocal microscopic images of Janus microgels for the encapsulation of NIH3T3 cells labelled using red and green cell trackers, respectively. Microgels are labelled with fluorescein and rhodamine to distinguish each compartment. Scale bars are 50 μm. D) Quantification of cell distribution in the separated compartments of the Janus microgels. E) Sorting result of cell-laden microgels containing green (FITC) or red (Texas red) cells using FACS. Scale bars are 20 μm. F) ALP staining for the microgels containing MSCs and/or HUVECs after 8 d coculture in a PDMS microwell (well diameter is 100 μm). To distinguish HUVEC from MSC, HUVEC cells are fluorescently labelled (green) before encapsulation. Positive ALP activity (fluorescently yellow) of MSC is observed with the close presence of HUVEC within the same microgel. Scale bar 100 um.

ADVANCED
SCIENCE NEWS
www.advancedsciencenews.com

NANO · MICRO
small
www.small-journal.com

$f(AB) = f(A) \times f(B)$, in which $f(A)$ and $f(B)$ represent the percentage of compartment in microgels containing only one single cell. We attain excellent correlation between experimental results and theoretical values of Poisson distribution for each type of cell at cell concentrations of 2.5×10^6 and 3.5×10^6 cell mL^{-1}. This is confirmed by our experiment which shows 24% of microgels containing red cells in green compartment and 17% of microgels containing green ones in red compartment, resulting into the pairing efficiency of ≈4.5% (Figure S4, Supporting Information). By further using fluorescence-activated cell sorting (FACS, BD FACSAria Cell Sorter), we categorize and collect microgels loaded with different cells according to the fluorescent characteristics of the cells (Figure 4E). We expect that the combination of the current cell microencapsulation method with available cell sorting techniques can enable scaled-up fabrication of multicompartment microgels containing various cell types of interest.[2a,13]

To demonstrate the feasibility of using multicompartment microgels as the platform to study single cell–cell interactions in vitro, we pair single stem cells with niche cells in Janus microgels. It has been previously shown that HUVECs can act as niche cells to accelerate the osteogenic differentiation of MSCs in conventional 2D dish-based coculture.[14] Here, we encapsulate MSCs (ATCC Number: PCS-500-012) and HUVECs (ANNGIO-PROTEMOMIE, cAP-0001RFP) within the Janus microgels and further seed the cell-laden microgels in PDMS microwells, thus avoiding the influence of cells from neighboring microgels.[15] By immunostaining with alkaline phosphatase (ALP) as an early marker for osteogenesis at 8 d after encapsulation, we observe positive ALP activity from MSCs paired with HUVECs (fluorescent green) within the same microgels, indicating osteogenic commitment of MSCs (Figure 4F). This indicates the potential regulatory effect of the interactions between MSCs and HUVECs on steering stem cell fate, reflecting the feasibility of the current approach as coculture platform for the study of intercellular communications.

In this paper, we present a simple and efficient one-step microfluidic approach to fabricate multicompartment microgels via rapid on-chip gelation of water-in-oil emulsion droplets consisting of multiple aqueous phases, followed by immediately transferring them into an aqueous buffer. This approach leads to the continuous production of multicompartment alginate microgels with high controllability over the structure and configuration of the microgels. Moreover, this strategy retains cell viability by avoiding prolonged exposure of cells to the oil phase during cell encapsulation. We demonstrate that our technique offers a biocompatible approach for studying cell–cell interaction at single cell level by pairing and coculturing single cells in a Janus microgel. This biocompatible microfluidic approach can be applied for controlled cell delivery by using different compartments for cells immobilization and targeted reorganization, and for directed bottom-up assembly of hierarchical tissue-like structure.[16]

Experimental Section

For all experimental details, please see Supporting Information.

Conflict of Interest

The authors declare no financial interests.

[1] a) M. P. Lutolf, P. M. Gilbert, H. M. Blau, *Nature* **2009**, *462*, 433; b) D. Steinhilber, T. Rossow, S. Wedepohl, F. Paulus, S. Seiffert, R. Haag, *Angew. Chem., Int. Ed.* **2013**, *52*, 13538; c) H. N. Joensson, H. Andersson Svahn, *Angew. Chem., Int. Ed.* **2012**, *51*, 12176; d) Y. F. Li, N. Khuu, A. Gevorkian, S. Sarjinsky, H. Therien-Aubin, Y. H. Wang, S. H. Cho, E. Kumacheva, *Angew. Chem., Int. Ed.* **2017**, *56*, 6083.

[2] a) T. Frank, S. Tay, *Lab Chip* **2015**, *15*, 2192; b) Y.-C. Chen, Y.-H. Cheng, H. S. Kim, P. N. Ingram, J. E. Nor, E. Yoon, *Lab Chip* **2014**, *14*, 2941; c) R. Wieduwild, S. Krishnan, K. Chwalek, A. Boden, M. Nowak, D. Drechsel, C. Werner, Y. Zhang, *Angew. Chem., Int. Ed.* **2015**, *54*, 3962.

[3] a) C.-H. Choi, S.-M. Kang, S. H. Jin, H. Yi, C.-S. Lee, *Langmuir* **2015**, *31*, 1328; b) S. Jiang, Q. Chen, M. Tripathy, E. Luijten, K. S. Schweizer, S. Granick, *Adv. Mater.* **2010**, *22*, 1060; c) K. Maeda, H. Onoe, M. Takinoue, S. Takeuchi, *Adv. Mater.* **2012**, *24*, 1340; d) A. C. Misra, S. Bhaskar, N. Clay, J. Lahann, *Adv. Mater.* **2012**, *24*, 3850; e) Y. Du, E. Lo, S. Ali, A. Khademhosseini, *Proc. Natl. Acad. Sci. USA* **2008**, *105*, 9522; f) E. Tumarkin, L. Tzadu, E. Csaszar, M. Seo, H. Zhang, A. Lee, R. Peerani, K. Purpura, P. W. Zandstra, E. Kumacheva, *Integr. Biol.* **2011**, *3*, 653; g) Q. Chen, S. Utech, D. Chen, R. Prodanovic, J.-M. Lin, D. A. Weitz, *Lab Chip* **2016**, *16*, 1346; h) S. Seiffert, *Angew. Chem., Int. Ed* **2013**, *52*, 11462.

[4] a) F. Guilak, D. M. Cohen, B. T. Estes, J. M. Gimble, W. Liedtke, C. S. Chen, *Cell Stem Cell* **2009**, *5*, 17; b) T. Rossow, J. A. Heyman, A. J. Ehrlicher, A. Langhoff, D. A. Weitz, R. Haag, S. Seiffert, *J. Am. Chem. Soc.* **2012**, *134*, 4983.

[5] a) D. Dendukuri, D. C. Pregibon, J. Collins, T. A. Hatton, P. S. Doyle, *Nat. Mater.* **2006**, *5*, 365; b) D. Dendukuri, S. S. Gu, D. C. Pregibon, T. A. Hatton, P. S. Doyle, *Lab Chip* **2007**, *7*, 818.

[6] a) S. Utech, R. Prodanovic, A. S. Mao, R. Ostafe, D. J. Mooney, D. A. Weitz, *Adv. Healthcare Mater.* **2015**, *4*, 1628; b) W. H. Tan, S. Takeuchi, *Adv. Mater.* **2007**, *19*, 2696; c) S. Hong, H. J. Hsu, R. Kaunas, J. Kameoka, *Lab Chip* **2012**, *12*, 3277; d) Y. Deng, N. Zhang, L. Zhao, X. Yu, X. Ji, W. Liu, S. Guo, K. Liu, X. Z. Zhao, *Lab Chip* **2011**, *19*, 4117; e) H. Huang, X. He, *Appl. Phys. Lett.* **2014**, *105*, 143704; f) H. Huang, M. Sun, T. Heisler-Taylor, A. Kiourti, J. Volakis, G. Lafyatis, X. He, *Small* **2015**, *11*, 5369.

[7] I. Akartuna, D. M. Aubrecht, T. E. Kodger, D. A. Weitz, *Lab Chip* **2015**, *15*, 1140.

[8] S. Zhao, W. Wang, M. Zhang, T. Shao, Y. Jin, Y. Cheng, *Chem. Eng. J.* **2012**, *207*, 267.

[9] a) J. Clausell-Tormos, D. Lieber, J.-C. Baret, A. El-Harrak, O. J. Miller, L. Frenz, J. Blouwolff, K. J. Humphry, S. Köster, H. Duan, *Chem. Biol.* **2008**, *15*, 427; b) Y. Tsuda, Y. Morimoto, S. Takeuchi, *Langmuir* **2010**, *26*, 2645.

[10] C.-H. Choi, H. Wang, H. Lee, J. H. Kim, L. Zhang, A. Mao, D. J. Mooney, D. A. Weitz, *Lab Chip* **2016**, *16*, 1549.

[11] D. Noudeh, P. Khazaeli, S. Mirzaei, F. Sharififar, S. Nasrollahosaiani, *J. Biol. Sci.* **2009**, *9*, 423.

[12] A. Wenger, A. Stahl, H. Weber, G. Finkenzeller, H. G. Augustin, G. B. Stark, U. Kneser, *Tissue Eng.* **2004**, *10*, 1536.

[13] M. Cordey, M. Limacher, S. Kobel, V. Taylor, M. P. Lutolf, *Stem Cells* **2008**, *26*, 2586.

[14] a) D. Kaigler, P. H. Krebsbach, E. R. West, K. Horger, Y.-C. Huang, D. J. Mooney, *FASEB J.* **2005**, *19*, 665; b) Y. Xue, Z. Xing, S. Hellem, K. Arvidson, K. Mustafa, *Biomed. Eng. Online* **2009**, *8*, 1.

[15] a) S. Gobaa, S. Hoehnel, M. Roccio, A. Negro, S. Kobel, M. P. Lutolf, *Nat. Methods* **2011**, *8*, 949; b) A. B. Bernard, C.-C. Lin, K. S. Anseth, *Tissue Eng., Part C* **2012**, *18*, 583; c) M. Charnley, M. Textor, A. Khademhosseini, M. P. Lutolf, *Integr. Biol.* **2009**, *1*, 625.

[16] Q. Chen, S. C. Bae, S. Granick, *Nature* **2011**, *469*, 381.